$$Z_m = X_m + Y_m$$

$$U_m^{(1)} = I_1(t) + P_m$$

$$W_m^{(1)} = U_m^{(1)} + V_m$$

$$\bar{Q}_n = \bar{\beta}_{3yn} \cot\left(\bar{\beta}_{3yn} p\right)$$

$$\bar{R}_n = \bar{\beta}_{2yn} \cos\left(\bar{\beta}_{2yn} b\right)$$

$$\bar{S}_n = \bar{Q}_n \sin\left(\bar{\beta}_{2yn} b\right)$$

$$\bar{T}_n = \bar{\beta}_{2yn} \sin\left(\bar{\beta}_{1yn} p\right)$$

$$\bar{P}_n = \frac{\beta_{2yn} I_2(t) + Q_n \bar{I}_3(t)}{\bar{R}_n + \bar{S}_n} \sin\left(\bar{\beta}_{1yn} p\right)$$

$$\bar{U}_n = \bar{I}_1(t) - \bar{P}_n$$

$$\bar{V}_n = \frac{\bar{T}_n \bar{I}_4(t)}{\left(\bar{R}_n + \bar{S}_n\right) \sin\left(\bar{\beta}_{3yn} p\right)}$$

$$\bar{W}_n = \bar{U}_n - \bar{V}_n$$

$$\bar{X}_n = \bar{\beta}_{1yn} \bar{I}_5(t) - \left[ - \frac{\bar{\beta}_{2yn} \bar{I}_6(t) + \bar{Q}_n \bar{I}_7(t)}{\bar{R}_n + \bar{S}_n} \right] \sin\left(\bar{\beta}_{1yn} p\right)$$

$$\bar{Y}_n = \frac{\bar{\beta}_{3yn} \bar{T}_n \bar{I}_8(t)}{\left(\bar{R}_n + \bar{S}_n\right) \sin\left(\bar{\beta}_{3yn} p\right)}$$

$$\bar{Z}_n = \bar{X}_n - \bar{Y}_n$$

$$\alpha_t = \begin{cases} 1, & \text{if } t \neq 0 \\ 3, & \text{if } t = 0. \end{cases}$$

## REFERENCES


[1] E. A. J. Marcatili, "Dielectric rectangular waveguide and directional coupler for integrated optics," *Bell Syst. Tech. J.*, vol. 48, pp. 2071–2102, Sept., 1969.

[2] R. M. Knox and P. P. Toulios, "Integrated circuits for the millimeter through optical frequency range," in *Proc. Symp. Submillimeter Waves* (New York, NY), Mar. 31–Apr. 2, 1970.

[3] R. M. Knox and P. P. Toulios, "A *V*-band receiver using image line integrated circuits," in *Proc. Nat. Electronics Conf.*, Oct. 16–18, 1974, Paper V 29, pp. 489–492.

[4] W. V. McLevige, T. Itoh, and R. Mittra, "New waveguide structure for millimeter wave and optical integrated circuits," *IEEE Trans. Microwave Theory Tech.*, vol. MTT-23, pp. 788–794, Oct. 1975.

[5] R. M. Knox, "Dielectric waveguide: A low cost option for IC's," *Microwaves*, vol. 15, pp. 56–57, Mar. 1976.

[6] R. Rudokas and T. Itoh, "Passive millimeter wave IC components made of inverted strip dielectric waveguides," *IEEE Trans. Microwave Theory Tech.*, vol. MTT-24, pp. 978–981, Dec. 1976.

[7] T. Itoh, "Inverted strip dielectric waveguide for millimeter wave integrated circuits," *IEEE Trans. Microwave Theory Tech.*, vol. MTT-24, pp. 821–827, Nov. 1976.

[8] T. Itoh and B. Adelseck, "Trapped image guide for millimeter wave circuits," *IEEE Trans. Microwave Theory Tech.*, vol. MTT-28, pp. 1433–1436, Dec. 1980.

[9] J. A. Paul and Y. W. Chang, "Millimeter wave image guide integrated passive devices," *IEEE Trans. Microwave Theory Tech.*, vol. MTT-26, pp. 751–754, Oct. 1978.

[10] T. Yoneyama and S. Nishida, "Nonradiative dielectric guide for millimeter wave integrated circuits," *IEEE Trans. Microwave Theory Tech.*, vol MTT-22, pp. 1188–1192, Nov. 1981.

[11] S. Shindo and T. Itanami, "Low-loss rectangular dielectric image line for millimeter-wave integrated circuits," *IEEE Trans. Microwave Theory Tech*, vol. MTT-26, pp. 747–751, Oct. 1978.

[12] K. Solbach and I. Wolff, "Electromagnetic fields and phase constants of dielectric image lines," *IEEE Trans. Microwave Theory Tech.*, vol. MTT-26, pp. 266–274, Apr. 1978.

[13] R. Mittra *et al.*, "Analysis of open dielectric wave guides using mode matching technique and variational method," *IEEE Trans. Microwave Theory Tech.*, vol. MTT-28, pp. 36–43, Jan. 1980.

[14] R. F. Harrington, *Time Harmonic Electromagnetic Fields*. New York: McGraw-Hill, 1961.


# A Method of Avoiding the Edge Current Divergence in Perturbation Loss Calculations

LEONARD LEWIN, FELLOW, IEEE

*Abstract*—**From a consideration of the properties near the edge of a flat finite-thickness strip and an elliptic cross-section strip, it is shown that the divergence that arises in the perturbation method near a sharp edge can be handled by halting the loss calculation at a definite distance just short of the strip edge. This distance can be expressed in terms of the radius of curvature at the tip for a rounded edge, and in terms of the strip thickness for a flat edge.**

## I. INTRODUCTION

A commonly used loss calculation method proceeds by taking the tangential magnetic field, as determined for the lossless case, calculating first the surface currents on the metal boundaries and then calculating the loss from these currents on the assumption that they are not affected substantially in form by the finite metal conductivity. The method can be applied if the metal thickness is everywhere sufficiently greater than the skin depth, and can even be used for infinitely thin strips or diaphragms when the very small amount of thickness that would be needed to appreciably exceed the skin depth would not alter the field substantially from the theoretical value in the ideal (zero-thickness) case. The one place where this cannot be done is for the axial current along a strip edge, since the ideal current density near the edge varies as $r^{-1/2}$, where $r$ is the distance from the edge. For this variation, the needed square of the current density varies as $1/r$ and produces a logarithmic divergence if integrated to the strip edge at $r = 0$. Since all such strips, in practice, have a certain thickness, and often a slightly rounded edge, an examination of the local fields in such cases may be expected to show how to deal with the divergence.

One method of avoiding this divergence altogether is to simply assume a finite thickness and to carry out the usually much more involved analysis for the thick-strip case. This has been done by Cockroft [1] for isolated rectangular conductors, and by Kaden [2] for a microstrip configuration. The problem with this method is that it requires a *major* change in the field calculations just in order to accommodate a local feature in the immediate neighborhood of the edge. Nosich and Shestopalov [3], assuming a rounded edge of diameter equal to the strip thickness, noted that the magnetic field from a cylinder of radius $w$ varies as $1/kw$, so that the actual field near the edge singularity should not become greater than this. They therefore stop the integration short by the requisite amount, of the order of $(kw)^2$, where $k = 2\pi/\lambda$. Not only is this truncation limit somewhat indefinite, but it is also frequency dependent, and assumes that the edge is rounded like a circular cylinder.

When the analysis for the nonzero thickness case is available, there is, in fact, no need to utilize the perturbation method at all; and Wheeler [4], using a technique based on an "incremental inductance" concept, showed how the losses could be calculated more directly. However, since the purpose of this paper is to be able to use the zero-thickness analysis, and to *avoid* extending it to the nonzero thickness case, it does not seem possible to adapt Wheeler's method for this purpose, since the needed normal derivative is not available.

Manuscript received May 11, 1983; revised February 7, 1984.

The author is with the Electromagnetics Laboratory, Department of Electrical and Computer Engineering, University of Colorado, Boulder, CO 80309.

0018-9480/84/0700-0717$01.00 ©1984 IEEE

A more precise analysis, combining the technique used by Cockroft with the truncation method of Nosich and Shestopalov, enables the calculations with the ideal (zero-thickness) fields to be used, with only a minor modification to take the edge features into account. Moreover, since the effect is a very local one, in the immediate proximity of the edge, a quasi-static examination of a suitable canonical problem should be sufficient to show the essential features, providing the result can be expressed in terms of local geometrical parameters only.

## II. Conformal Transformation

If an infinite strip of suitable cross section is examined as a quasi-static problem, the stream function $U$ and the potential $V$ are related to the coordinates $x$ and $y$ by an equation of the form

$$x + iy = F(U + iV) \tag{1}$$

where $F$ is an analytic function which can be determined from the shape of the cross section. If $n$ is a variable along the direction of the outward normal and $s$ a variable along the cross-section surface, then, for a TEM wave, $\partial V/\partial n$ and $\partial U/\partial s$ are, respectively, proportional to the normal electric field and the tangential magnetic field at the cross section. The latter, at the boundary surface, is proportional to the axial current density. Hence, the loss perturbation calculation involves the integral $\int I^2\,ds \propto \int (\partial U/\partial s)^2\,ds = \int (\partial U/\partial s)\,dU$ taken between appropriate limits. The use to be made of this formula is as follows:

i) Calculate the exact expression for a finite-thickness strip,
ii) calculate the limiting form of the expression for an infinitely thin strip where the integration stops just short of the edge,
iii) by comparing i) and ii) above, determine how far short of the edge one should stop the integration in order to equal the exact result for the finite-thickness strip, and
iv) put this result in terms of local geometric parameters only.

If step iv) can be achieved, what results is a construction for using the infinitely thin strip analysis to obtain results corresponding to a thin nonzero thickness strip, thus permitting the perturbation analysis to proceed even in this case.

The method will be illustrated for the cases of a flat edge (thin rectangular strip) and a rounded edge (thin elliptic strip).

## III. Flat Edge

Fig. 1 shows a flat edge with the coordinate $x$ varying from 0 to some value $D$ large enough that local conditions at $x = D$ do not affect appreciably the field near $x = 0$. The $y$ coordinate at the edge varies from 0 to $-L$ and the conformal transformation between $z = x + iy$ and $W = U + iV$ comes from integrating $dz/dw = C(W^2 - 1)^{1/2}$ and determining the constants so that $z = 0$ corresponds to $W = 1$; $z = -iL$ to $W = -1$. Thus the rectangular strip itself is the equipotential $V = 0$ and the integration gives

$$\pi z/L = W(W^2 - 1)^{1/2} - \log\left[W + (W^2 - 1)^{1/2}\right]. \tag{2}$$

At $V = 0$ on the strip surface, this gives the following:

a) *Upper surface*, $y = 0, 0 < x < D$:

$$\pi x/L = U(U^2 - 1)^{1/2} - \log\left[U + (U^2 - 1)^{1/2}\right], \qquad 1 < U < U_0 \tag{3}$$

where $U_0 = (\pi D/L)^{1/2} + O(D^{-1/2})$ for large $D$.

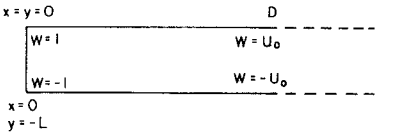


Fig. 1. Rectangular strip cross section.

b) *Vertical surface*, $x = 0, -L < y < 0$:

$$\pi y/L = U(1 - U^2)^{1/2} - \cos^{-1} U, \qquad -1 < U < 1. \tag{4}$$

c) *Lower surface*, $y = -L, 0 < x < D$:

$$\pi x/L = -U(U^2 - 1)^{1/2} - \log\left[-U + (U^2 - 1)^{1/2}\right], \qquad -U_0 < U < -1. \tag{5}$$

The required integrations give the losses $P_1$ proportional to

$$\begin{aligned} P_1 &= \int_1^{U_0} \frac{dU}{dx}\,dU + \int_{-1}^{1} \frac{dU}{dy}\,dU + \int_{-1}^{-U_0} \frac{dU}{dx}\,dU \\ &= \frac{\pi}{2L}\left\{2\int_1^{U_0} \frac{dU}{(U^2 - 1)^{1/2}} + \int_{-1}^{1} \frac{dU}{(1 - U^2)^{1/2}}\right\} \\ &= \frac{\pi}{2L} \log\left(\frac{4\pi e^{\pi} D}{L}\right) + O(D^{-1/2}). \end{aligned} \tag{6}$$

The corresponding equation for an infinitely thin strip to give $x = D$ at $U = U_0$ is

$$\pi x/L = U^2. \tag{7}$$

If we take the lower integration limit to $x = d$, the corresponding loss calculation gives

$$P_2 = 2\int_{U_1}^{U_0} \frac{dU}{dx}\,dU = \frac{\pi}{L}\int_{U_1}^{U_0} \frac{dU}{U} = \frac{\pi}{L} \log \frac{U_0}{U_1} \tag{8}$$

where $U_0 = (\pi D/L)^{1/2}, U_1 = (\pi d/L)^{1/2}$. Hence

$$P_2 = \frac{\pi}{2L} \log \frac{D}{d}. \tag{9}$$

Comparing this with (6) gives

$$d = L/(4\pi e^{\pi}) \approx L/290. \tag{10}$$

Thus the usual loss calculation can be made and will yield a result equal to that for a thin strip if the integration is taken to a distance from the strip edge of approximately one three-hundredth of the strip thickness. It may be noted that (10) is "local" in the sense that the extension $D$ does not enter into the expression.

## IV. Rounded Edge

Fig. 2 shows a rounded edge as one apex of an elliptic cross section of semi-axes $a$ and $b$. The radius of curvature at this apex is

$$R = b^2/a. \tag{11}$$

The coordinates and the potentials are related by

$$x + iy = A \sin(U + iV) \tag{12}$$

where $A$ is a scale factor. From (12)

$$\begin{aligned} x &= A \sin U \cosh V \\ y &= A \cos U \sinh V \end{aligned} \tag{13}$$

and the equation of an ellipse at potential $V_0$ is

$$\frac{x^2}{A^2 \cosh^2 V_0} + \frac{y^2}{A^2 \sinh^2 V_0} = 1. \tag{14}$$

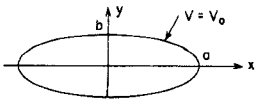


Fig. 2. Elliptic cross-section strip.

Hence

$$A\cosh V_0 = a \quad A\sinh V_0 = b$$

giving

$$\tanh V_0 = b/a. \tag{15}$$

If the ellipse degenerates into an infinitely thin strip, then $b = 0$ and $V_0 = 0$. For nonzero thin strips, $b/a$ will be small, as will $V_0$, and we shall be concerned with very small, but nonzero, values of $V_0$.

The element $ds = [(dx)^2 + (dy)^2]^{1/2} = AdU[\cosh^2 V_0 - \sin^2 U]^{1/2}$ from (13). Hence the loss associated with the ellipse is proportional to

$$P_3 = \int_0^{2\pi} \frac{dU}{ds}\, dU = \frac{4}{A}\int_0^{\pi/2} \frac{dU}{\left[\cosh^2 V_0 - \sin^2 U\right]^{1/2}}$$

$$= \frac{4}{a} K(1/\cosh V_0) \tag{16}$$

where $K$ is the complete elliptic integral of the first kind. For $V_0$ small the modulus is close to unity, and (16) has the expansion

$$P_3 = \frac{4}{a}\log(4\coth V_0) + O(V_0^2) \approx \frac{4}{a}\log(4a/b). \tag{17}$$

For an infinitely thin strip, $V_0 \to 0$, $x \to a\sin U$ and the losses are given by

$$P_4 = 4\int_0^{a-d}\left(\frac{dU}{dx}\right)^2 dx = 4\int_0^{a-d}\frac{dx}{a^2 - x^2} \approx \frac{2}{a}\log\frac{2a}{d} \tag{18}$$

for small $d$.

Comparing with (17) gives

$$d = b^2/8a = R/8 \tag{19}$$

where $R = b^2/a$ is the radius of curvature at the apex. Again, this is a "local" result in that it depends only on geometrical parameters close to the edge. Because the width of an ellipse near its apex is quite ill-defined, it is not possible to relate this result directly to an equivalent strip thickness.

## V. Conclusions

The method of halting the loss integration a determinate distance just short of an edge enables loss perturbation calculations to be made with fields calculated for structures with infinitely thin strips or diaphragms. This should simplify such calculations considerably. The method encompasses a finite strip thickness with either a flat or rounded edge. In fact, the transformation of Section III would, if pursued to a potential surface $V_0 \neq 0$, be able to handle a variety of combinations of rounding and thickness.

## References

[1] J. D. Cockroft, "Skin effect in rectangular conductors at high frequencies," *Proc. Roy. Soc (London) Ser. A*, vol. 122, pp. 533–542, 1929.
[2] H. Kaden, "Advances in microstrip theory," *Siemens Forsch. u Entwickl. Ber.*, vol. 3, no. 2, pp. 115–124, 1974.
[3] A. I. Nosich and V. P. Shestopalov, "Ohmic losses in transmission lines with thin conductors," *Sov. Phys. Dokl.*, vol. 25, pp. 127–128, Feb. 1980.
[4] H. A Wheeler, "Formulas for the skin effect," *Proc. IRE*, vol. 30, pp. 412–424, 1942.

# A Technique for the Design of Microwave Transistor Oscillators

K. L. KOTZEBUE

***Abstract*—A technique for the design of microwave transistor oscillators is presented in which measurements made on an experimentally optimized amplifier are used to calculate six basis oscillator circuits which yield maximum power output. The procedure has been experimentally verified by the construction of a silicon bipolar transistor test oscillator at 1 GHz.**

## I. Introduction

A microwave transistor power amplifier is often easier to optimize experimentally than the corresponding microwave transistor oscillator. A transistor power amplifier is easily optimized because, at a given frequency and operating point, only two parameters need be varied: the input RF drive level, and the output load impedance (assuming that harmonic impedance terminations are not of first-order importance). Once these parameters are experimentally optimized, the design is completed by measuring the input impedance and constructing an input matching network. In the case of the transistor oscillator, however, there are a multitude of possible oscillator configurations, each more difficult to experimentally optimize for maximum power output than an amplifier. It is more difficult to experimentally optimize an oscillator for maximum power output because of the relatively large number of interacting circuit elements which must be varied, while maintaining a condition of oscillation. But since we know that a transistor operates under the same set of RF voltages and currents when delivering its maximum added power as an amplifier as it does when delivering its maximum output power as an oscillator, it should be possible to take information obtained from an easily optimized power amplifier and use this information to calculate optimum oscillator configurations. In this paper, such a design procedure is presented.

## II. Design Procedure

The first step in the procedure is to experimentally optimize the large-signal performance of the transistor by varying the load impedance and RF drive level until the transistor's added power has been maximized. The load may be varied in the conventional fashion using stub tuners, etc., or the load may be synthesized by injecting a second signal into the output port in the manner reported by Takayama [1]. The incident and reflected waves $a_1$, $b_1$, $a_2$, and $b_2$, as shown in Fig. 1, can be measured on a network analyzer setup, and the added power computed from (1)

$$\text{Power} = |b_2|^2\left\{1 - \frac{1}{|S'_{22}|^2} - \frac{1-|S'_{11}|^2}{|S'_{21}|^2}\right\} \tag{1}$$

where

$$S'_{11} \equiv \frac{b_1}{a_1}$$

$$S'_{22} \equiv \frac{b_2}{a_2}$$

$$S'_{21} \equiv \frac{b_2}{a_1}.$$

0018-9480/84/0700-0719$01.00 ©1984 IEEE